

An Ising Model of Bursts and Fizzles in Intergroup Violence

Jeroen Bruggeman*, Don Weenink, Bram Mak

Abstract

During intergroup confrontations, agitating stimuli such as opponents' threats and provocations can trigger collective violence. We examine video recordings of street fights between groups of young men. Collective violence sometimes breaks out in a burst and at other times in a fizzle wherein only few group members participate. These two patterns are accurately predicted by an Ising model with asymmetric spins.

1 Introduction

The centennial Ising spin glass model has been applied to a wide range of phenomena [29, 26], among others in social life [1, 19, 7, 10, 32, 15]. One important social phenomenon—cooperation for public goods—has been rarely studied by this model, however, because the symmetry of the spin values (-1 and 1) mismatches the asymmetry of defection (D) and cooperation (C). Although a complicated workaround is possible for a two-person public goods game [1], we obtain a simpler and more general model by abandoning the symmetry.

Our purpose is to predict and explain when, how, and in what kind of pattern collective action commences, in particular in violent conflicts. In our empirical data, the public good of a group is the victory over, or the defense against, opponents. Our subjects are unarmed and not professionally trained fighters, with limited ability to estimate their payoffs. Collective action in uncertain situations, such as (potentially) violent confrontations, has been explained by models of thresholds [17], cascades [34], and critical mass [23]. These models are built on the assumption that initiative takers or leaders

*Corresponding author: Jeroen Bruggeman, j.p.bruggeman@uva.nl

initiate cooperation. Threshold and critical mass models also depend on the assumption that participants have (nearly) perfect information about the numbers of defectors and cooperators. The Ising model does not rely on these assumptions, and is therefore more parsimonious. Individuals only have information about their network neighbors. At a confrontation, focal group members are agitated by opponents' provocations, threats, and movements—turmoil, in short—that corresponds to temperature in the original model. Due to turmoil, one or few individuals may accidentally start cooperating (fighting, in our case), called “trembling hands” in game theory [12]. This effect happens to be embedded in the Metropolis algorithm [6] used to solve the Ising model [3]. When few individuals start cooperating, they influence their network neighbors, and when turmoil passes a critical level, there is a burst of cooperation. In answering the how question, the Ising model thus points out that cooperation can start by accidental cooperators who are agitated, rather than exceptionally zealous and/or well-informed individuals. If there are initiative takers or leaders, however, they can be accommodated [5].

The novelty of this paper is in its prediction of the temporal unfolding of collective action. When a group consists of unconditional defectors, who are unresponsive to turmoil and cooperating network neighbors, and conditional cooperators [8], who cooperate if they are agitated and/or enough others cooperate, in proportion $p : 1 - p$, respectively, there is a critical level p_c that separates two different patterns. If $p \leq p_c$, collective action breaks out in a burst, whereas if $p > p_c$, there is no burst but a fizzle of few group members who contribute asynchronously. Furthermore, small groups and small clusters in large groups are more easily agitated to cooperate than large groups, starting at lower levels of turmoil. The predicted proportion, p_c , and the size effect are strongly supported by video recorded street fights.

2 Ising model

Network ties (coupling) and spins (behavior) are defined differently than in the usual Ising model [29, 26]. Network tie $A_{ij} > 0$ means that individual i is in close proximity of and pays attention to group member j , or else $A_{ij} = 0$. We assume that attention is reciprocal but not necessarily equal. Because attention is scarce and people tend to respond to proportions of their social environment rather than absolute numbers [34], ties are row-normalized, $w_{ij} = A_{ij} / \sum_{j=1}^n A_{ij}$, with n the size of the group. A group member can contribute to the public good, with behavioral variable $S_i = C$, or defect, $S_i = -D$, and $0 < D < C$. With row-normalization and

asymmetric spins, our Ising model [6] is the Hamiltonian

$$H = - \sum_{i \neq j} w_{ij} S_i S_j. \quad (1)$$

In our examples and empirical study, we choose $C = 1$. For the dilemma of cooperation to be nontrivial, D must be chosen such that H has a global minimum when the number of cooperators, $N_C = n$, and a single maximum in between $N_C = 0$ and $N_C = n$ (Fig. 1). We chose $D = 1/2$ in an earlier paper [6] to maximally distinguish D from the trivial values $D = 1$ and $D = 0$.

Fig. 1 plots H/n with N_C/n for group sizes $n = 2$ and $n = 5$. The hill is a graphical representation of the dilemma of collective action.

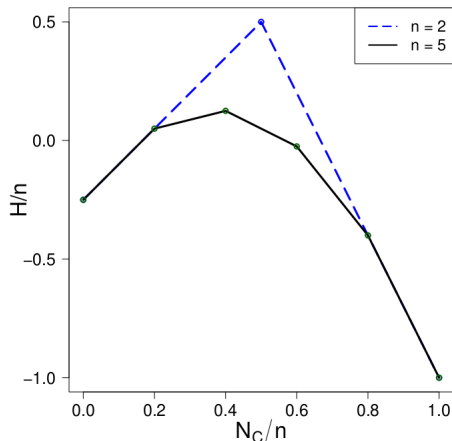


Figure 1: The dilemma of collective action presented as a hill in between full defection (left) and full cooperation (right), with the proportion of cooperators (N_C/n) on the horizontal axis; $C = 1$ and $D = 1/2$. The vertical axis (H/n) could be intuited as a negative likelihood; moving uphill from a state of defection ($N_C/n = 0$) is very unlikely. A proportion of unconditional defectors, p , means that even if all conditional cooperators contribute, $N_C/n \leq 1 - p$.

We do not assume that individuals know their payoffs in advance, but they will heuristically—and perhaps wrongly—distinguish between valuable ($C > D$) and unvaluable ($C < D$) public goods. Payoffs are defined to facilitate interpretation, but they play no role in solving the model. The payoff for a cooperator is the same as in evolutionary game theory [30]; when an actor cooperates among N_C other cooperators, $P_C = \theta(N_C + 1)/n - 1$, with

an enhancement factor $\theta \geq 1$. A defector's payoff is almost the same as in game theory, $P_D = \theta N_C/n + Q$, except for a factor Q , which establishes that P_D approximates P_C when D approximates C [$Q = (\theta/n - 1)(1 - R)$; $R = (C - D)/(C + D)$]; and $\theta = \theta_0 + R$ with a base rate $\theta_0 \geq 1$.

The values of D and C can be related to the familiar symmetric Ising model through a mapping

$$\{-D, C\} \rightarrow \{S_0 - \Delta, S_0 + \Delta\} \quad (2)$$

with a bias $S_0 = (C - D)/2$ with respect to 0. Then, the two behavioral options become symmetrical with respect to S_0 at an offset $\pm\Delta$. It has been shown that the asymmetry of S is equivalent to the symmetric model ($S_0 = 0$) with an external field $2S_0$ [6]. If Δ is set to a fixed value (0.75 in our examples), decreasing S_0 makes cooperation less valuable, and is equivalent to an increasing threshold of cooperating network neighbors to win actors over to cooperate, also in other binary decision models [34, 17]. A case in point is an opponent group that is (much) larger than the focal group. Cooperation becomes more appealing when S_0 increases, which corresponds to a decreasing threshold or proportion of cooperating network neighbors. This happens, for example, when group members overestimate their fighting skills.

The dynamics of a group are driven by agitating stimuli, T , analogous to temperature in the original model. In our empirical study, T expresses the (aggregated) effect of opponents on members of a focal group. Initially, all focal group members defect. If $p = 0$ and T increases past a critical level T_c , there is a burst of cooperation wherein the majority of group members participates (Fig. 2). If p increases, T_c increases, and the proportion of participants in the burst (N_C/n) decreases; if $p > p_c$, the bursty pattern does not appear. Fighting ends when exhaustion sets in, a winner stands out, or others intervene. To determine p_c , we will conduct a mean field analysis.

3 Mean field analysis

For the mean field analysis, the proportion of cooperators, N_C/n , is expressed in terms of the order parameter, $M = 1/n \sum_{i=1}^n S_i$. Consequently, $N_C/n = (M + D)/(C + D)$.

The mean field assumption can be stated as $S_i = \bar{S}_i = M$. Starting out with the Hamiltonian (Eq. 1), using the mapping from Eq. 2, taking the row-normalization of the adjacency matrix into account, and leaving out the

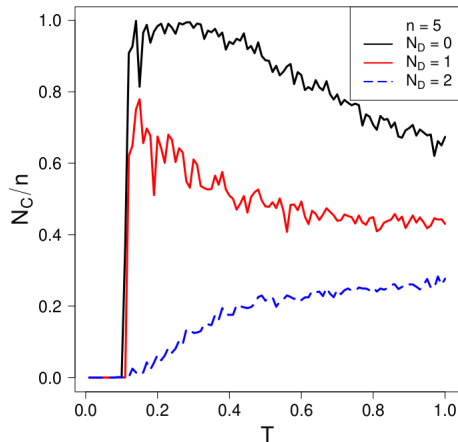


Figure 2: (Color online.) Proportion of cooperators (N_C/n) with agitation (T) in a fully connected network in the size range of our empirical study ($n = 5$); $C = 1$ and $D = 1/2$. The black line depicts the group without unconditional defectors ($p = 0$), the red line with one unconditional defector ($p < p_c$), and the dashed blue line with two unconditional defectors ($p > p_c$).

Boltzmann constant, it has been established [6] that

$$M = S_0 + \Delta \tanh(\Delta M/T). \quad (3)$$

Here, we distinguish unconditional defectors, in proportion p , from conditional cooperators, $1 - p$. Accordingly,

$$M = S_0 - p\Delta + (1 - p)\Delta \tanh(\Delta M/T). \quad (4)$$

Identifying critical T (see Supplementary Material) leads to

$$\begin{aligned} & -\frac{\operatorname{arcosh}(\sqrt{\Delta^2(1-p)/T})}{\Delta^2/T} + \\ & (1-p)\sqrt{1 - \frac{1}{\Delta^2(1-p)/T}} = \frac{S_0}{\Delta} - p. \end{aligned} \quad (5)$$

Solutions of this equation become complex if $p > \frac{S_0}{\Delta}$, hence $p \leq \frac{S_0}{\Delta}$. The choice of $C = 1$ and $D = 1/2$ implies that there is no (burst of) cooperation if $p > 1/3$. We are now to find out what the mean field result tells us about actual street fights.

4 Empirical study

Bystanders often film street violence with their phones, and upload their videos to websites such as YouTube, LiveLeak, and WorldStarHipHop, where we collected our data. Our sample from these sites is not random with respect to violence, hence we cannot test if turmoil is its cause, but in all likelihood it is random with respect to the temporal patterns of violence. We analyzed 59 groups in the size range $2 \leq n < 10$ (and one larger group, with six active members); see Supplementary Material for details and examples. The videos were coded using Noldus Observer XT 14 software. Videos were played at half speed many times over. Each of 406 individuals was coded for belonging to a focal, opponent, or third-party group. Their behavior was interpreted and represented on the timeline.

4.1 Operationalization

We coded *violence* when force was used against another’s body (punching, slapping, kicking, hitting, stomping) and/or when another person’s body was forcefully moved. People may defect (not use violence) for all kinds of reasons and due to various causes. Yet, *unconditional defectors* have in common that they are (temporarily) inactive while others contribute. Among them we include deescalators, as well as group members who were prevented to fight by deescalators.

We subsumed the following behaviors of members of the opponent group under *turmoil* for the focal group: aggressing, including fighting gestures; pulling off clothing (jackets or vests); pulling up pants; pointing toward opponents; provocative gesturing with fingers or hands (as an invitation to engage); bending forward toward an opponent; encroaching (invading opponents’ personal space through using or damaging objects belonging to them); teasing, such as lightly hitting or ridiculing; and violence. Because over small time intervals, turmoil accumulates in participants’ minds, we calculated the level of turmoil from the beginning of the video until a focal group’s (first) maximum participation in violence, by multiplying the duration of each instance of turmoil by the number of individuals involved, and adding up all these weighted instances. This scale should be improved in future studies, but our main prediction is independent of it.

Given the distraction caused by turmoil, it is not feasible for all group members to react within 1 second to a first cooperator, as in a well-organized sports team, whereas 3 seconds is too long for the notion of burst to apply to our small groups. Hence we defined a *burst* as an outbreak of violence by at least half of the group (Fig. 2), or both individuals in a dyad, if they started

fighting less than 2 seconds after the first, with a 5% margin.

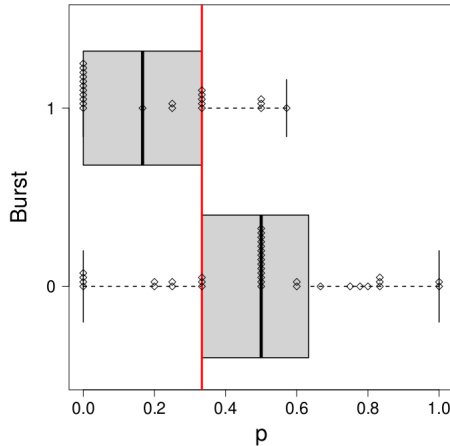


Figure 3: The proportion of unconditional defectors, p , and the predicted critical level p_c (based on $C = 1$ and $D = 1/2$) as vertical line, with box-plots of bursts (1) and fizzles (0).

4.2 Empirical results

Of the 59 groups considered, there were 23 groups where violence started in a burst, 15 groups where violence was collective without a burst, and 21 cases of violence by a single group member, thus no burst either. The proportions of defectors in groups with bursts ($\bar{p} = 0.19$; $\text{sd} = 0.21$) and groups without bursts ($\bar{p} = 0.49$; $\text{sd} = 0.27$) are box-plotted in Fig. 3 (Welch test $t = 4.796$; $P = 6.411 \cdot 10^{-6}$; $\text{df} = 54.76$). The critical level of $p_c = 1/3$, drawn as vertical line in Fig. 3, separates most of the bursts from the nonbursts, although some groups are on the wrong side of the line.

Turmoil preceded all collective violence with one exception, where two individuals suddenly assaulted a passive victim. As said, we have no accurate scale for turmoil, and our assessment is tentative. Moreover, T_c is case-specific, co-depends on group size, both in absolute number [5] and relative to the size of the opponent group, and increases with p (up to p_c). Consistent with simulations [5], we found that cooperation in small groups tends to start at lower turmoil than in larger groups ($\text{cor.} = 0.53$) and in the latter, it tends to start in small subgroups. This bottom up mounting of cooperation is similar to bottom up synchronization in the Kuramoto model [2]. The size-turmoil relation is slightly disturbed by dyad-groups more often facing

larger opponent groups, and therefore being less likely to fight than triads. As a matter of fact, larger groups always defeated smaller opponent groups (made them flee or worked them to the ground) with only one exception.

5 Conclusions

With asymmetric spins, the Ising model explains when (T_c), how (Metropolis), and in what pattern (burst/fizzle) collective violence commences, without recourse to initiative takers [17], perfect information [23], or traditional explanations based on reputations [27], prosocial norms [13], or feedback through selective incentives [28]. The traditional mechanisms are recent in evolutionary history, whereas agitating stimuli are billions of years old. Therefore the model might also be useful in biology, for example to study quorum sensing bacteria [11]. The model can be applied to cooperation in other domains of human collective action, such as street protests [16] or helping victims [31]. For different domains, specific scales of agitating stimuli will have to be developed, which will be easier for lab experiments than field studies. If required, the model can incorporate norms (as external fields), selective incentives (through individualized $S_{0,i}$), and noisy reputations [4]. In all likelihood, more discoveries lay ahead.

Data and code accessibility

All coded videos and the R-script used to produce graphs thereof are available at <https://osf.io/f25nq/>

—Supplementary Material—

Data and compilation of data set

In contrast to prior studies of violence and deescalatory action based on CCTV footage [20, 21, 31] most of our videos were captured on mobile phones, which tend to provide better picture clarity, detail and sound. Whereas CCTV footage is most often shot from an elevated and fixed camera angle, people who record violent incidents on their mobile phones tend to follow the action, thereby allowing us to observe bodily positioning and movements in more detail [22].

One concern about phone-recorded clips is that recorders start filming when the antagonism is already ongoing; our data are thus left-truncated to an unknown degree. We discarded footage that immediately started with physical violence. Another concern is that uploaded videos might be biased toward more spectacular cases. However, our sample shows variety in the forms and severity of violence, ranging from groups who engage in frenzied collective violence to incidents that involve just a few slaps. A third concern is whether the recording influenced the behavior of the assailants. Several videos showed more than one person recording the incident. Earlier work [?] noted that a host of research indicates that people do not change their behavior substantially in the presence of a camera and mainly focus on what they are doing. This is probably even more the case in antagonistic situations, and because young people are used to being filmed by phones. Additionally, when people do pay attention to the camera, which happened in just one of our clips, it is visible in the recording and can be incorporated in the analysis. (In our case, this concerned behavior coded as turmoil.)

We used the following criteria to compile our dataset. First, we only included incidents in which at least one of the antagonistic parties comprised at least two members. Second, we only selected clips in which violence could be observed from the (or a) beginning until the end. Third, we focused on fights that seemed to have occurred spontaneously, excluding prearranged fights on the basis of any of the following criteria: the fighters and bystanders all had approximately the same young age (e.g., school yard fights); the antagonists were wearing protective clothing; or a referee was present. Regarding gender, the overwhelming majority of the incidents were between males, with only 8 cases involving both females and males. We excluded female-only fights because they often seemed being arranged (back yard fights with male referees).

Along these criteria, we obtained 42 videos from websites such as YouTube, LiveLeak, and WorldStarHipHop, using search terms with the English key-

words “brawl,” “street fight,” and “assault.” This sample appears to be random with respect to temporal unfolding and (sub)group size. 36 clips are from English-speaking countries (mainly the US and the UK, with one from Canada and one from India); 5 of the remaining clips are from the Netherlands, and 1 is from Colombia. We did not observe differences in relevant behavior related to the location of the recording.

The shortest clip lasted 30 sec. and the longest nearly 5 minutes (mean 101 sec.; s.d. 59 sec.). Out of a potential 2×42 groups, where the opponents in one analysis become the focal group in the next, 25 groups fought with a single individual rather than a group, which leaves $\mathcal{N}=59$ groups to examine. Most groups were small, $2 \leq n < 10$ (mean 3.6), but one had 14 members (of which 6 became violent). The smaller ones were simulated as fully connected networks wherein everyone could see one another unless there were obstacles or deescalators obstructing visual contact. Obstruction was simulated by removing m ties.

Ethics

The use of videos for research purposes poses distinct ethical challenges, largely due to the non-anonymous content of the videos. However, ethical guidelines for digital spaces tend to be less restrictive [25], with the consent of the participants being less stringent for data acquired from the public domain, including the internet. While our video corpus is open to use and inspection by other researchers upon request, we require that they take the same measures to ensure the anonymity of the persons portrayed as we did.

Coding

We used Noldus Observer XT 14 software to code the behaviors of individuals, resulting in start times and durations of behaviors per individual throughout the video clip. The software distinguishes state events of relatively longer duration (e.g., holding a person) from point events that are brief single acts (e.g., a punch). When an act of violence took a more extended duration (e.g., holding or dragging), we coded the entire duration of the act, thus creating a state event. When a series of violent point events appeared less than two seconds after one another, we connected them, thus creating a state event.

To enhance the precision of our coding, we coded observable actions (such as kicking, punching, pointing at opponent) and later lumped them together to generate the main codes: violence, turmoil, and deescalation. We coded

the behavior of each actor in multiple rounds, coding only one type of action per round. The video material was played at half speed and repeated many times, which is important because violence proceeds too fast to see what is going on in real time. The first 20 clips were coded by one of the authors and two assistants. We discussed the coding when we disagreed and continued the procedure by multiple coders until agreement was reached. At this point, the remainder of the clips were coded by one (meanwhile) experienced assistant researcher and were later checked by another. The remaining disagreements or mistakes were discussed, and the coding was adjusted accordingly.

To identify whether individuals belonged to a focal, opponent, or third-party group, we observed whether they remained close (at touching distance) to each other as they moved through space, whether they called each other by their names, whether they touched each other (for instance, by tapping shoulders), or whether they shared a vehicle or other object (for instance, a bag or skateboard). One of the authors and two assistants discussed each case in which we observed one or more of these behaviors to determine whether the actors were part of the same group.

Composition of indicators

Violence. We coded violence when members of the focal group used force against another’s person’s body (by punching, slapping, kicking, hitting, stomping) and/or when actors moved or held another person’s body forcefully (by pushing, shoving, dragging, wrestling, holding, etc.). To enhance the reliability of our coding, we also coded whether actors used their hands, legs, or other body parts (e.g., elbow, head) and whether weapons were used, including the type of weapon, excluding guns (i.e., knives, sticks, tasers and improvised weapons, such as a skateboard or bottle, etc.). We define collective violence as time intervals wherein two or more members of the focal group used violence simultaneously, either as overlapping state events or, in fewer cases, as simultaneously occurring point events. The maximum participation in collective violence was determined by taking the largest number of focal group members engaging in violent action, divided by the total number of focal group members.

In the videos, it was not possible to distinguish leaders from initiative takers, but we noticed individuals who started violence on their own. In simulations, a leader/initiative taker i can be incorporated by a larger, individual $S_{0,i}$ value; the result is collective action at lower T .

Unconditional defectors do not cooperate when $T \geq T_c$ or most network neighbors cooperate. First, we labeled as unconditional defectors, the focal

group members who took deescalatory action towards others. Their behavior was coded as follows [20]: open-handed gestures in the direction of other individuals; waving arms to stop or dampen in the direction of others; touching or patting; guiding a person away; pulling people apart; and putting one's body in between opponents. Whether deescalators' interventions were effective or not, they were at least temporarily unavailable to participate in violence themselves, and their behavior signaled noncooperation to their fellow group members. Second, we noted group members who were effectively stopped from using violence for at least five seconds by other focal group members, opponents, or third-party members (e.g., bystanders). Third, group members remaining passive when others fought. Fourth, group members unable to participate in violence due to spatial constraints for at least five seconds, for instance, due to cars blocking their way or because they were not close enough to the action. Fifth, group members unable to participate for at least five seconds because they were wounded or had fallen to the ground. We took all five reasons for and causes of defection into account for the proportion of unconditional defectors before and during the first instance of violence by the focal group.

Turmoil. We subsumed the following behaviors of members of the opponent group under the heading of turmoil for the focal group. First, we coded approaching when opponents moved closer to focal group members. We also indicated whether actors moved energetically (jumping/skipping) and whether they ran. Second, aggressive behaviors when actors in the opponents' group moved body parts in a way that signaled provocation, hostility and/or a readiness to attack. We used the following modifiers (sub-codes) to specify aggressing behavior: fighting gestures; pulling off clothing (jackets or vests); pulling up pants; pointing at opponents; provocative gesturing with fingers or hands (as an invitation to engage); bending forward (head and/or chest bending toward opponent); encroaching (invading opponents' personal space through using or damaging objects belonging to them); and teasing (invading opponents' body space in a teasing/ridiculing way that does not inflict bodily harm, such as lightly hitting, stroking, or patting the opponent's body). Third, involuntary behavior that increases the vulnerability of opponents, because it tends to agitate (signaling opportunity) and provoke violence. This concerned stumbling and falling to the ground. Finally, violence committed by members of the opponent group. Because we do not know the psychological impact of the various kinds of turmoil, we could not construct a ratio level scale. Instead, we calculated the total level of turmoil from the beginning of the clip until a focal group's maximum participation in violence by noting the duration of each instance of turmoil, and multiplying it by the number of opponents involved, i.e., the surface area under the

turmoil curve in Fig. 7, 10, and S11.

Bursts. We identified bursts when, at the first moment of collective violence, two conditions are fulfilled: (1) at least half of the focal group members joined the fight, or both actors did in a dyad, and (2) cooperators started fighting in less than 2 seconds (with a 5% margin) after the first. Condition (1) follows from simulations of small groups; see Table 3 and Fig. 13. Note that in simulations of much larger networks ($n \geq 1000$), bursts can occur wherein less than half of a group participates. In some videos, we observed multiple bursts; in these cases, we only considered the first burst to facilitate comparison of cases.

Alternative explanation of collective action

A plausible alternative explanation of the onset of collective action is synchrony of motion [24], which yields a feeling of oneness among group members [14] and a stronger willingness to take risks for one's group mates [33].

We measured the synchronization of focal group members pairwise if they engaged in the following behaviors simultaneously (i.e., overlapping intervals on the timeline). Approaching members of the opponent group at the same pace (normal, energetic, or running), distancing from the opponent group at normal walking speed (we consider simultaneous distancing at energetic or running pace uncontrolled attempts to escape rather than forms of synchrony), or simultaneously engaging in any of the forms of aggressing (above). To calculate the level of synchrony, we noted the duration of each instance of synchrony from the beginning of the clip prior to the moment of maximum participation in violence, and we multiplied it by the proportion of focal group ties involved (i.e., normalized with respect to the maximum number of ties in the group).

Although in 21 out of 23 bursts, some degree of synchronization preceded collective violence, there were 18 cases in which synchronization was not followed by collective violence. In some of the latter cases, synchrony turned out to be a deceptive performance composed of blustering and aggrandizing without commitment to fighting. This does not imply that synchronization is unimportant (it probably is for solidarity [9]), but it just does not predict collective violence.

Examples from videos

Graphs of behavior on the timeline enable to analyze and compare the coded videos. Each graph shows the intervals and their durations of (collective) violence, turmoil, synchrony and deescalation (see Fig. 7, 10, 11).

To illustrate, we discuss how coded video data was turned into a graph for clip 26. Fig. 4-6 feature screenshots of the clip, and Fig. 7 displays the graph. This clip features a confrontation of a dyad (focal group) with a triad (opponents) in a restaurant. Violence started at approximately 14 seconds into the video and quickly became collective until approximately 28 seconds. Four instances of turmoil preceded the violence, starting with one of the members of the opponent group gesturing aggressively and walking around in a jumpy, energetic way. The members of the focal dyad walked synchronously toward and away from the opponent in three shorter and one relatively longer stretch of time. Fig. 4 captures a moment of synchrony; the members of the dyad were making fighting gestures and stood aligned, each stretching out one leg with their feet pointing toward the opponent, and the other leg standing backward. Fig. 5 shows the moment when the dyad's level of agitation reached a critical level; when one of the focal actors dodged backward, avoiding being hit, his companion was about to deliver a blow to the head of the opponent, which made the latter fall down. Fig. 6 displays the second member of the opponents' triad (soon joined by the third) rushing into the restaurant toward the focal dyad, near his fallen companion. At this point, both groups were engaged in collective violence. Fig. 5 also shows bystanders (who can be seen sitting at a table in Fig. 4) and employees standing near the counter. At 28 seconds, an employee took deescalatory action for the first time. At that point, the collective violence had stopped already and erupted again for a shorter moment approximately 2 seconds later. The clip ends when two triad members carry their fallen group member outside. By then, the focal dyad had already left the scene.

Fig. 8-10 provide another illustration. Fig. 10 is the graph of clip 86; it shows three outbreaks of collective violence in a group of five members who faced a single opponent. In the first instance of collective violence (not a burst by our 2 seconds criterion), starting at approximately 60 seconds into the clip and lasting for approximately 30 seconds, four members participated. Three of them immediately followed each other, and the fourth joined after approximately 2 seconds. Prior to the outbreak of violence, the opponent agitated focal group members by walking back and forth and by posturing aggressively. Fig. 8 captures the trigger moment of agitation; i.e., while



Figure 4: Still taken from clip 26 at 0:06 seconds.



Figure 5: Still taken from clip 26 at 0:13 seconds.

one member of the focal group was engaged in aggressive posturing and a group member tried to deescalate, the opponent was about to strike another focal group member. Fig. 9 shows the situation 4 seconds later, when three members of the focal group were attacking.



Figure 6: Still taken from clip 26 at 0:15 seconds.

Analysis of coded and plotted videos

We used graphs of coded videos in our analysis, illustrated in Fig. 11, where the opponent group in clip 67 is plotted. The horizontal axis is the timeline in thousands of seconds, the vertical axis is the proportion of group members involved (for turmoil and violence), and the proportion of intragroup ties involved out of the maximum possible number of ties (for synchrony of action). The first moment of collective violence, denoted by the downward arrow, involves two focal group members. There is, however, a short interruption of collective violent action. Therefore, we did not code this occurrence of collective violence as a burst. The time gap between the first participant and maximum participation in collective violence, denoted by the horizontal arrows, takes over 6 seconds.

In the figure, seven instances of turmoil occur (numbered 1-7) prior to the moment of maximum participation in violence: (1) a short interval that, after a brief interruption, continues for 4 seconds and involves 67% of the opponent group (2 members); (2) involves all three members of the opponent group and lasts nearly 1 second; (3) lasts less than 1 second and involves 33% of the opponent group; (4) turmoil continues, with an intermittent short dip, for over 1 second with 67% involvement; (5) a peak at 100% involvement that lasts less than 1 second; (6) a short drop to 67% involvement that takes approximately 1 second; (7) the last turmoil before maximal violence. We

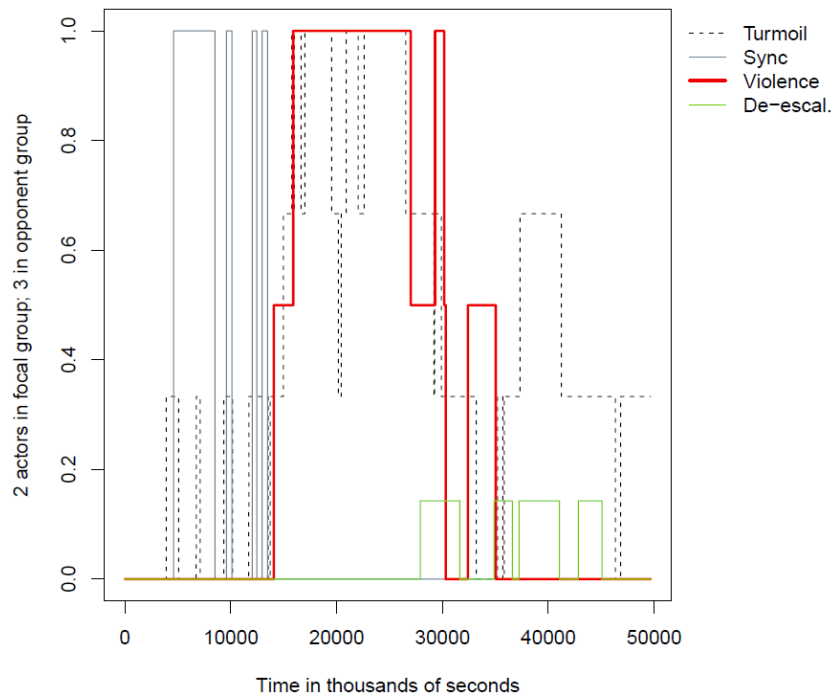


Figure 7: Graph of clip 26 with a burst of collective violence in a dyad.



Figure 8: Still taken from clip 86 at 0:59 seconds.

calculated the level of turmoil by multiplying the time length of each of these intervals by the number of actors involved.

Intervals of synchrony in Fig. 11 are indicated by A and B. A lasted



Figure 9: Still taken from clip 86 at 1:03 seconds.

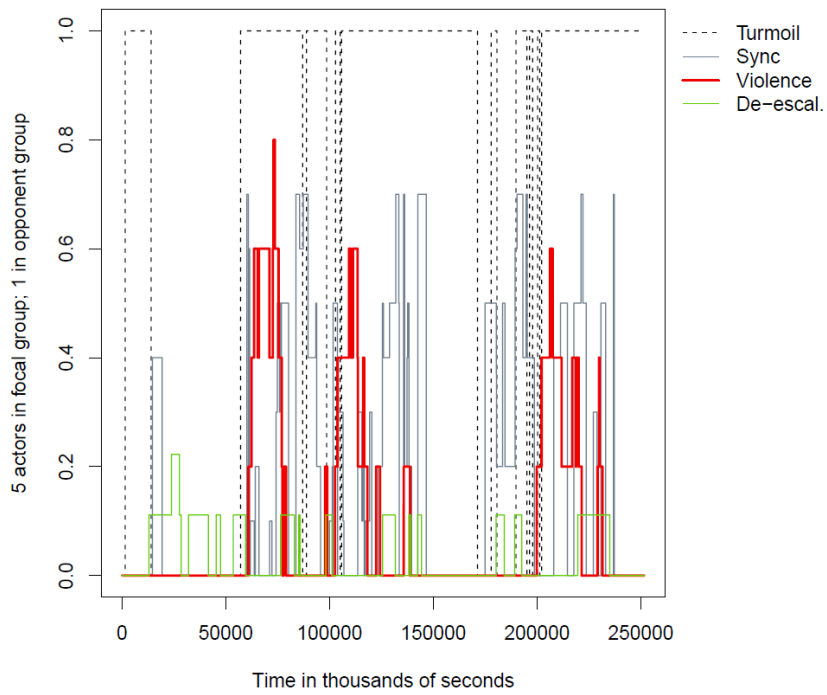


Figure 10: Graph of clip 86. Outbreaks of collective violence in a group of five. Because the time between the first and last participant's commencement of violence exceeds 2 seconds, these outbreaks are not classified as bursts.

2.4 seconds and involved all ties in the group; B involved 67% of the ties for approximately 2 seconds prior to maximum participation in violence. Finally, the graph shows intervals of deescalatory action.

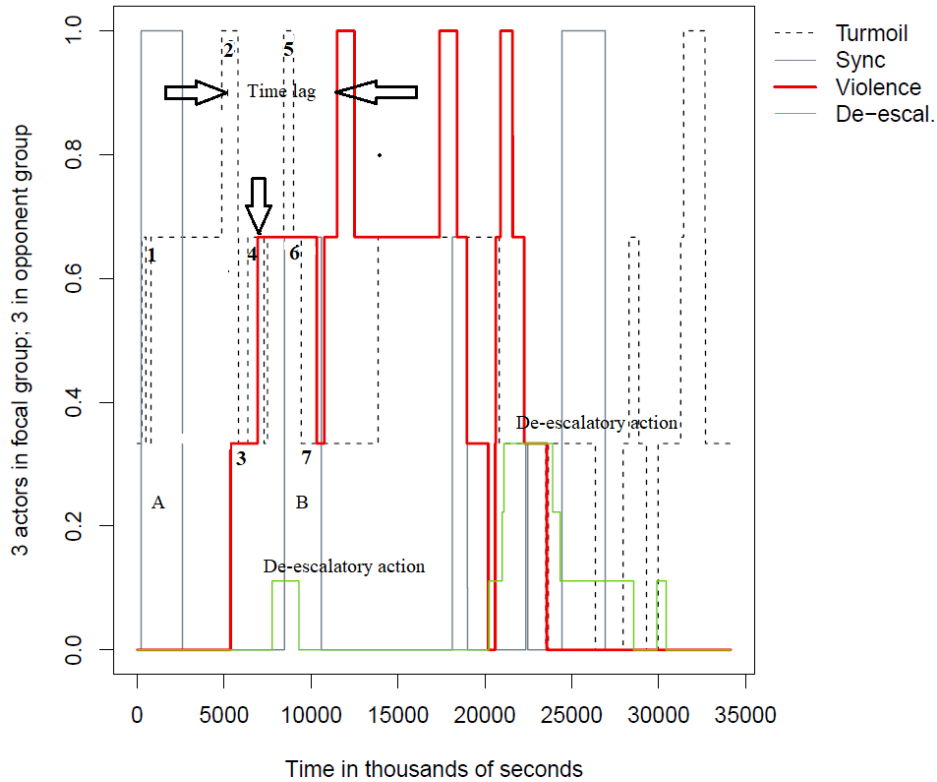


Figure 11: Graph of clip 67; opponent group. The timeline displays the start of collective violent action (downward arrow), instances of turmoil (1-7), synchrony (A,B), the time lag between the first and last group member joining the collective violence (horizontal arrows), and deescalatory action.

The 21 groups where only a single member fought

Of the 21 groups where violence was committed by a single member, 13 were dyads. In 11 of these 21 groups, one or few deescalators in the focal group successfully prevented participants from using violence. In 2 groups,

members of the opponent group were able to avoid collective violence by hampering focal group members from joining the fight. In 2 dyads, the participants were separated by their opponents and could not adjust their actions to each other any longer, leaving them to either fight on their own or flee. All these outcomes are consistent with the Ising model once interrupted ties and/or unconditional defectors are simulated. In 4 of the 6 remaining groups, opponents carried knives, a machete, a bat, or looked too intimidating even when unarmed, which apparently lowered S_0 in the focal groups. In the remaining 2 groups, members took turns attacking a fallen victim instead of using violence simultaneously, perhaps confident that they were in control (low uncertainty; high S_0). Because we took the same S_0 values for all conditional cooperators, variations of these values are below the resolution of our simple model, though.

Overview of cases and descriptive statistics

Our dataset contains information about the behavior of 406 individuals in 42 violent incidents. The 59 groups and their key characteristics are listed in Table 1. After focal and opponent groups have been analyzed as listed, they flip roles with respect to cooperation and turmoil production in a second batch of the analysis, except when an opponent is solitary instead of a group.

| | group | n | c.v. | N_C | lag | burst | T | Sync | N_D |
|----|---------------------------|-----|------|-------|-------|-------|-------|--------|-------|
| 1 | 1_beachfight_focal | 3 | 1 | 2 | 0.00 | 1 | 0.97 | 19.39 | 1 |
| 2 | 3_asianeateries_focal | 5 | 0 | 1 | | 0 | 72.41 | 18.10 | 4 |
| 3 | 3_asianeateries_oppon. | 2 | 0 | 1 | | 0 | 93.37 | 16.20 | 1 |
| 4 | 6_rikshaddrivers_focal | 6 | 1 | 4 | 1.93 | 1 | 7.24 | 5.33 | 2 |
| 5 | 7_baldies_focal | 4 | 1 | 3 | 0.92 | 1 | 6.42 | 0.94 | 1 |
| 6 | 8_queensday_focal | 14 | 1 | 6 | 1.95 | 1 | 45.81 | 303.42 | 8 |
| 7 | 9_gasstation_focal | 2 | 0 | 1 | | 0 | 14.49 | 16.30 | 1 |
| 8 | 10_redpickup_focal | 3 | 1 | 3 | 0.93 | 1 | 9.34 | 78.75 | 0 |
| 9 | 26_insideeatery_focal | 3 | 1 | 3 | 1.21 | 1 | 14.41 | 0.20 | 0 |
| 10 | 26_inseeatery_oppon. | 2 | 1 | 2 | 1.77 | 1 | 7.49 | 5.32 | 0 |
| 11 | 27_dallasairport_focal | 6 | 1 | 5 | 0.00 | 1 | 24.99 | 3.53 | 1 |
| 12 | 32_shovedbycar_focal | 3 | 1 | 2 | 3.66 | 0 | 3.66 | 0.00 | 1 |
| 13 | 41_kababshop_focal | 2 | 0 | 1 | | 0 | 42.12 | 0.00 | 1 |
| 14 | 41_kababshop_oppon. | 2 | 1 | 2 | 0.84 | 1 | 5.90 | 0.42 | 0 |
| 15 | 45_onbusystreet_focal | 2 | 1 | 2 | 1.48 | 1 | 12.79 | 9.35 | 0 |
| 16 | 50_fitness_focal | 2 | 1 | 2 | 3.08 | 0 | 4.62 | 1.54 | 0 |
| 17 | 52_blockingskaters_focal | 2 | 0 | 1 | | 0 | 20.44 | 10.72 | 1 |
| 18 | 52_blockingskaters_oppon. | 4 | 0 | 1 | | 0 | 45.56 | 17.36 | 3 |
| 19 | 53_famousonyoutube_focal | 2 | 1 | 2 | 20.23 | 0 | 14.45 | 0.00 | 1 |
| 20 | 53_famousonyoutube_opp. | 2 | 0 | 1 | | 0 | 51.11 | 0.00 | 1 |
| 21 | 54_hammeronhead_focal | 4 | 1 | 3 | 1.57 | 1 | 9.17 | 4.19 | 1 |
| 22 | 54_hammeronhead_oppon. | 2 | 1 | 2 | 1.57 | 1 | 31.43 | 5.24 | 0 |

| | | | | | | | | | |
|----|------------------------------|---|---|---|-------|---|--------|-------|---|
| 23 | 60_gangattack_focal | 6 | 0 | 1 | | 0 | 31.73 | 80.43 | 5 |
| 24 | 61_burgerking_focal | 2 | 0 | 1 | | 0 | 37.88 | 0.00 | 1 |
| 25 | 66_guyvsgang_focal | 6 | 1 | 6 | 1.81 | 1 | 0.91 | 19.22 | 0 |
| 26 | 67_poolfight_focal | 3 | 1 | 2 | 0.84 | 1 | 16.46 | 4.36 | 1 |
| 27 | 67_poolfight_oppon. | 3 | 1 | 3 | 6.29 | 0 | 19.87 | 2.49 | 1 |
| 28 | 84_brokenwindow_focal | 3 | 0 | 1 | | 0 | 35.36 | 2.89 | 2 |
| 29 | 86_tables_focal | 5 | 1 | 4 | 2.25 | 0 | 29.23 | 4.50 | 1 |
| 30 | 88_babypowder_focal | 2 | 1 | 2 | 2.10 | 1 | 5.43 | 4.20 | 0 |
| 31 | 92_didntdoanything_focal | 2 | 0 | 1 | | 0 | 46.51 | 8.35 | 1 |
| 32 | 93_groupkicking_focal | 4 | 1 | 3 | 5.92 | 0 | 8.68 | 10.02 | 1 |
| 33 | 95_apologise_focal | 9 | 1 | 2 | 1.51 | 0 | 26.42 | 76.30 | 7 |
| 34 | 95_apologise_oppon. | 2 | 0 | 1 | | 0 | 133.06 | 2.64 | 1 |
| 35 | 96_gangversusbat_focal | 6 | 0 | 1 | | 0 | 25.00 | 67.06 | 5 |
| 36 | 97_alleyfight_focal | 4 | 0 | 1 | | 0 | 61.14 | 26.32 | 4 |
| 37 | 97_alleyfight_oppon. | 4 | 1 | 2 | 0.76 | 1 | 34.39 | 3.83 | 2 |
| 38 | 98_stopmick_focal | 3 | 1 | 2 | 0.76 | 1 | 20.61 | 17.54 | 1 |
| 39 | 98_stopmick_oppon. | 2 | 0 | 1 | | 0 | 68.10 | 10.70 | 1 |
| 40 | 101_fightandrob_focal | 6 | 1 | 4 | 2.97 | 0 | 22.19 | 21.45 | 2 |
| 41 | 101_fightandrob_oppon. | 2 | 0 | 1 | | 0 | 79.09 | 3.10 | 1 |
| 42 | 104_waiting_focal | 4 | 1 | 4 | 0.73 | 1 | 13.83 | 0.36 | 0 |
| 43 | 104_waiting_oppon. | 2 | 0 | 1 | | 0 | 128.82 | 0.36 | 1 |
| 44 | 105_frenziassault_focal | 3 | 1 | 2 | 1.21 | 1 | 0.00 | 9.61 | 1 |
| 45 | 108_sidewalkbrawl_focal | 2 | 0 | 1 | | 0 | 268.40 | 44.73 | 1 |
| 46 | 108_sidewalkbrawl_oppon. | 4 | 1 | 2 | 0.00 | 1 | 33.55 | 36.72 | 2 |
| 47 | 110_nietklaar_focal | 5 | 1 | 3 | 14.45 | 0 | 36.13 | 12.04 | 1 |
| 48 | 121_eightballjacket_focal | 4 | 1 | 3 | 2.66 | 0 | 8.64 | 1.08 | 1 |
| 49 | 124_leavehimalone_focal | 3 | 1 | 3 | 4.86 | 0 | 13.36 | 0.00 | 0 |
| 50 | 124_leavehimalone_oppon. | 2 | 1 | 2 | 0.00 | 1 | 9.09 | 0.00 | 0 |
| 51 | 128_throwingfood_focal | 2 | 1 | 2 | 1.14 | 1 | 0.57 | 0.00 | 0 |
| 52 | 128_throwingfood_oppon. | 2 | 1 | 2 | 2.28 | 0 | 6.83 | 0.00 | 0 |
| 53 | 129_awayfrommyfood_focal | 5 | 1 | 2 | 3.06 | 0 | 14.22 | 4.09 | 3 |
| 54 | 129_awayfrommyfood_oppon. | 6 | 0 | 1 | | 0 | 65.37 | 30.00 | 5 |
| 55 | 133_homeboy_focal | 2 | 1 | 2 | 2.68 | 0 | 0.54 | 1.07 | 0 |
| 56 | 134_down_focalgroup | 4 | 1 | 2 | 0.89 | 1 | 23.12 | 45.27 | 2 |
| 57 | 134_down_oppon. | 5 | 1 | 2 | 0.89 | 0 | 40.02 | 9.34 | 3 |
| 58 | 138_cometomyhouse_focal | 3 | 0 | 0 | | 0 | 34.02 | 36.51 | 3 |
| 59 | 145_knifefightcolombia_focal | 2 | 0 | 1 | | 0 | 17.04 | 20.16 | 1 |

Table 1: Overview of all groups and their sizes; occurrence of collective violence (c.v.); maximum participation in violence (N_C); time lag between the first participant and maximum participation in collective violence; burst; levels of turmoil (T) and of synchrony at first violence outbreak; number of unconditional defectors (N_D). In group 8_queensday, two focal group members disappeared from view already before the first moment of violence had started; out of the remaining 12, 6 participated in collective violence.

Table 2 provides mean values, percentages, standard deviations, and minimum and maximum values for the indicators used in the analysis.

| | mean or n (%) | s.d. | min | max |
|---|-----------------|-------|------|--------|
| 1 Group size | 3.58 | 2.09 | 2 | 14 |
| 2 Dyads | 24 (40.7) | | 0 | 1 |
| 3 Triads | 11 (18.6) | | 0 | 1 |
| 4 Groups ≥ 4 members | 24 (40.7) | | 0 | 1 |
| 5 Collective violence | 38 (64.4) | | 0 | 1 |
| 6 Burst | 23 (39) | | 0 | 1 |
| 7 Maximum participation in violence | .64 | .28 | 0 | 1 |
| 8 Average time lag in bursts in sec. ($n = 23$) | 1.06 | .65 | 0 | 2.10 |
| 9 Average time lag per participant in non-bursts ($n = 15$) | 5.12 | 5.29 | 0.89 | 20.23 |
| 10 Turmoil prior to max participation in violence ($n = 38$) | 37 (97.4) | | 0 | 1 |
| 11 Level of turmoil prior to max part. in violence ($n = 38$) | 15.34 | 12.21 | 0 | 45.81 |
| 12 Synchrony prior to max part. in violence ($n = 38$) | 32 (84.2) | | 0 | 1 |
| 13 Level of synchrony prior to max part. in violence ($n = 38$) | 18.98 | 50.95 | 0 | 303.42 |
| 14 Proportion unconditional defectors | .37 | .28 | 0 | 1.0 |

Table 2: Descriptive statistics of indicators used in the analysis ($\mathcal{N}=59$). Note: Levels of synchrony prior to maximum violence includes an outlier of 303.42. Without outlier, mean = 11.29; s.d. = 18.96; max = 78.75. We excluded this outlier in the calculations reported.

Solving the Ising model

The Ising spin glass model can be solved computationally by the Metropolis algorithm (next subsection). First, it is solved analytically by a mean field analysis for $p = 0$. The case when $p > 0$ is analyzed in the main text.

Mean field analysis

For the mean field analysis, we assess the level of cooperation, N_C/n , in terms of the order parameter, $M = 1/n \sum_{i=1}^n S_i$. Consequently, $N_C/n = (M + D)/(C + D)$. The mean field assumption can be stated as $S_i = \hat{S}_i = M$. For the moment, the proportion of unconditional defectors, $p = 0$; see below when $p > 0$.

We start out with the Hamiltonian, $H = -\sum_{i,j} w_{ij} S_i S_j$. We use the mapping $\{C, -D\} \rightarrow \{S_0 + \Delta, S_0 - \Delta\}$ with bias $S_0 = (C - D)/2$ and offset $\Delta = (C + D)/2$ to rewrite the Hamiltonian as

$$H = -\sum_{i,j} w_{ij} (S_0 + \hat{S}_i)(S_0 + \hat{S}_j), \quad (6)$$

with \hat{S}_i and $\hat{S}_j \in \{-\Delta, \Delta\}$, and taking into account the row-normalization of the adjacency matrix ($\sum_j^n w_{ij} = 1$) [6].

To calculate the Boltzmann probabilities of a single spin (or an individual's probabilities to cooperate or defect), we define the pertaining Hamiltonian

$$H_i = - \sum_j w_{ij} (S_0 + \hat{S}_i)(S_0 + \hat{S}_j) \quad (7)$$

$$\begin{aligned} H_i &= - \sum_j w_{ij} (S_0 + \hat{S}_i) M \\ &= -(S_0 + \hat{S}_i) M \\ H_i^\pm &= -S_0 M \mp \Delta M. \end{aligned} \quad (8)$$

In the subsequent derivation, we use no Boltzmann constant (and no β either), just T . The average value of a spin, \bar{S}_i , according to the Boltzmann distribution, with $P(S_i^-)$ standing for the probability that S_i is negative and $P(S_i^+)$ that it is positive, is

$$\begin{aligned} \bar{S}_i &= S^- P(S_i^-) + S^+ P(S_i^+) \quad (9) \\ &= \frac{S^- e^{-H_i^-/T} + S^+ e^{-H_i^+/T}}{e^{-H_i^-/T} + e^{-H_i^+/T}} \\ &= \frac{S^- e^{-(-S_0 M + \Delta M)/T} + S^+ e^{-(-S_0 M - \Delta M)/T}}{e^{(-S_0 M + \Delta M)/T} + e^{(-S_0 M - \Delta M)/T}} \\ &= \frac{S^- e^{-\Delta M/T} + S^+ e^{\Delta M/T}}{e^{-\Delta M/T} + e^{\Delta M/T}} \\ &= \frac{(S_0 - \Delta) e^{-\Delta M/T} + (S_0 + \Delta) e^{\Delta M/T}}{e^{-\Delta M/T} + e^{\Delta M/T}} \\ &= S_0 \frac{e^{-\Delta M/T} + e^{\Delta M/T}}{e^{-\Delta M/T} + e^{\Delta M/T}} + \Delta \frac{-e^{-\Delta M/T} + e^{\Delta M/T}}{e^{-\Delta M/T} + e^{\Delta M/T}} \\ &= S_0 + \Delta \tanh(\Delta M/T). \end{aligned} \quad (10)$$

So far, we only dealt with conditional cooperators, but in our empirical study, there are also unconditional defectors in proportion $p > 0$. Accordingly, we define M_{cc} as the average spin value of the conditional cooperators and M_{ud} as the average spin value of the unconditional defectors. Note that $M_{ud} = S^-$. We assume that the unconditional defectors are homogeneously distributed across the network. Accordingly, the mean field equation becomes

$$S_i = p S^- + (1 - p) M_{cc}. \quad (11)$$

The Hamiltonian for a single conditional cooperators becomes

$$H_i^\pm = -(S_0 \pm \Delta)(pS^- + (1-p)M_{cc}) \quad (12)$$

$$= -S_0pS^- \mp \Delta pS^- - S_0(1-p)M_{cc} \mp \Delta(1-p)M_{cc}. \quad (13)$$

In the derivation of Eq. 10, all terms that did not contain $\mp\Delta$ canceled each other out. For clarity, we remove these terms from Eq. 13, which results in

$$H_i^\pm = \mp\Delta(pS^- + (1-p)M_{cc}). \quad (14)$$

The mean field analysis for conditional cooperators i is

$$\begin{aligned} \bar{S}_i &= S^- P(S_i^-) + S^+ P(S_i^+) \\ &= \frac{S^- e^{-\Delta(pS^- + (1-p)M_{cc})/T} + S^+ e^{\Delta(pS^- + (1-p)M_{cc})/T}}{e^{-\Delta(pS^- + (1-p)M_{cc})/T} + e^{\Delta(pS^- + (1-p)M_{cc})/T}} \\ &= S_0 + \Delta \frac{-e^{-\Delta(pS^- + (1-p)M_{cc})/T} + e^{\Delta(pS^- + (1-p)M_{cc})/T}}{e^{-\Delta(pS^- + (1-p)M_{cc})/T} + e^{\Delta(pS^- + (1-p)M_{cc})/T}} \\ &= S_0 + \Delta \tanh(\Delta(pS^- + (1-p)M_{cc})/T) = M_{cc}. \end{aligned} \quad (15)$$

Using Eq. 11, we can express the self-consistency equation of M_{cc} in M ,

$$\begin{aligned} M &= pS^- + (1-p)(S_0 + \Delta \tanh(\Delta(pS^- + (1-p)M_{cc})/T)) \\ &= pS^- + (1-p)(S_0 + \Delta \tanh(\Delta M/T)) \\ &= S_0 - p\Delta + (1-p)\Delta \tanh(\Delta M/T). \end{aligned} \quad (16)$$

Critical proportion of unconditional defectors

Depending on T , the self-consistency equation has one unstable and two stable ferromagnetic solutions, or one stable paramagnetic solution. At a critical T , the system transitions between these two states. When the system is paramagnetic,

$$\frac{\partial}{\partial M}(S_0 - p\Delta + (1-p)\Delta \tanh(\Delta M/T)) < 1$$

at the solution of M . When the system is ferromagnetic,

$$\frac{\partial}{\partial M}(S_0 - p\Delta + (1-p)\Delta \tanh(\Delta M/T)) > 1$$

at the unstable solution of M . We can identify a critical T when

$$\frac{\partial}{\partial M}(S_0 - p\Delta + (1-p)\Delta \tanh(\Delta M/T)) = 1, \quad (17)$$

hence,

$$\begin{aligned}
\frac{1}{\cosh^2(\Delta M/T)} \Delta^2(1-p)/T &= 1 \\
\cosh(\Delta M/T) &= \sqrt{\Delta^2(1-p)/T} \\
\Delta M/T &= \pm \operatorname{arcosh}(\sqrt{\Delta^2(1-p)/T}) \\
\frac{M}{\Delta} &= \frac{\pm \operatorname{arcosh}(\sqrt{\Delta^2(1-p)/T})}{\Delta^2/T}. \quad (18)
\end{aligned}$$

We can substitute this expression (18) in the self-consistency equation (16)

$$\begin{aligned}
\frac{\pm \operatorname{arcosh}(\sqrt{\Delta^2(1-p)/T})}{\Delta/T} &= S_0 - p\Delta + (1-p)\Delta \tanh(\pm \operatorname{arcosh}(\sqrt{\Delta^2(1-p)/T})) \\
\frac{\pm \operatorname{arcosh}(\sqrt{\Delta^2(1-p)/T})}{\Delta^2/T} &= \frac{S_0}{\Delta} - p \pm (1-p) \tanh(\operatorname{arcosh}(\sqrt{\Delta^2(1-p)/T})) \\
&= \frac{S_0}{\Delta} - p \pm (1-p) \sqrt{1 - \frac{1}{\Delta^2(1-p)/T}}. \quad (19)
\end{aligned}$$

Discarding the equation that has no real numerical solutions leaves

$$-\frac{\operatorname{arcosh}(\sqrt{\Delta^2(1-p)/T})}{\Delta^2/T} + (1-p) \sqrt{1 - \frac{1}{\Delta^2(1-p)/T}} = \frac{S_0}{\Delta} - p. \quad (20)$$

Solutions of this equation become complex if $p > \frac{S_0}{\Delta}$, hence $p \leq \frac{S_0}{\Delta}$. Graphical illustrations are in Fig. 12. The choice of $C = 1$ and $D = 1/2$ implies that there is no (burst of) cooperation if $p > 1/3$.

Solving the Ising model computationally

Here, the Metropolis algorithm is used [3]. Surprisingly, p_c of simulated, fully connected networks is very close to the mean field calculation of p_c , even in very small networks; see Fig. 13. Given $C = 1$ and $D = 1/2$, there is no burst if $p_c > 0.34$. In simulations, p_c is proportionally less precise in smaller networks (Table 3), and the prediction for the triad (red dot in Fig. 13) is empirically false, whereas the mean field is correct: one unconditional defector does not prevent cooperation of the other two. Also one empirical group of six with two unconditional defectors had a burst, which did not happen in the simulations. The critical threshold is nearly density independent: if in (sufficiently large) simulated networks, density is decreased by two orders of magnitude, p_c increases from ≈ 0.34 to ≈ 0.35 . The degree distribution has no effect on p_c .

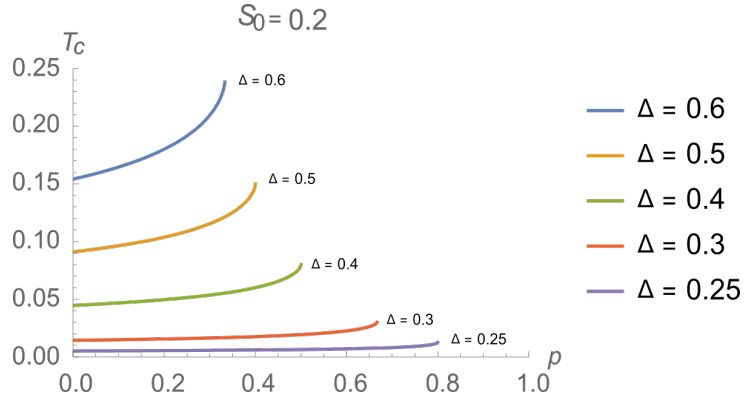


Figure 12: Given $S_0 = 0.2$, the critical level of agitation, T_c , is plotted as a function of the proportion of unconditional defectors, p , for various levels of Δ . The critical level, p_c , is reached at the right-hand end of the lines.

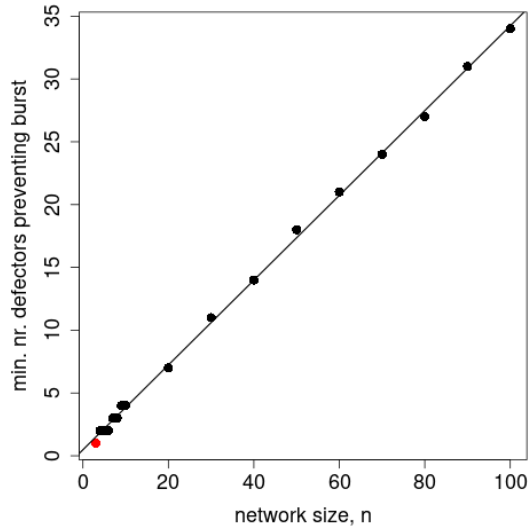


Figure 13: For simulated networks with sizes $3 \leq n \leq 100$, the minimum number of unconditional defectors who prevent a burst is plotted. The red dot marks the triad (1 defector prevents a burst), which conflicts with the empirical data (1 defector and a burst of 2).

| n | N_D | $\approx N_C$ | burst |
|-----|-------|---------------|-------|
| 2 | 1 | 0 | 0 |
| 3 | 1 | 1 | 0 |
| 4 | 1 | 2 | 1 |
| 5 | 1 | 3-4 | 1 |
| 6 | 1 | 4-5 | 1 |
| 5 | 2 | 1 | 0 |
| 6 | 2 | 2 | 0 |
| 7 | 2 | 4 | 1 |
| 8 | 2 | 4-5 | 1 |
| 9 | 2 | 6 | 1 |
| 9 | 3 | 3 | 0 |

Table 3: Simulations just below (burst = 1) and above (burst = 0) the critical threshold of unconditional defectors (N_D) in small groups (size n). The numbers of cooperators (N_C) fluctuate across simulation runs and are approximate. Note: For groups with $n = 7$ and $N_D = 2$, simulations in Fortran yield $N_C \approx 4$ whereas in R , $N_C \approx 3$.

Authors' contributions

JB made the asymmetric Ising model, and wrote the software and the paper. DW collected, interpreted, and analyzed the data. BM did the mean field analysis. JB and DW wrote the Supplementary Material.

References

- [1] Christoph Adami and Arend Hintze. Thermodynamics of evolutionary games. *Physical Review E*, 97:062136, 2018.
- [2] Alex Arenas, Albert Díaz-Guilera, and Conrad J. Pérez-Vicente. Synchronization reveals topological scales in complex networks. *Physical Review Letters*, 96:114102, 2006.
- [3] Alain Barrat, Marc Barthélemy, and Alessandro Vespignani. *Dynamical Processes on Complex Networks*. Cambridge University Press, New York, 2008.
- [4] Jeroen Bruggeman. *A Sociology of Humankind*. Routledge, New York, 2024.
- [5] Jeroen Bruggeman and Rudolf Sprik. Cooperation for public goods under uncertainty. *Lecture Notes in Computer Science*, 12140:243–251, 2020.
- [6] Jeroen Bruggeman, Rudolf Sprik, and Rick Quax. Spontaneous cooperation for public goods. *Journal of Mathematical Sociology*, 45:183–191, 2021.
- [7] Claudio Castellano, Santo Fortunato, and Vittorio Loreto. Statistical physics of social dynamics. *Reviews of Modern Physics*, 81:591, 2009.

- [8] Ananish Chaudhuri. Sustaining cooperation in laboratory public goods experiments. *Experimental Economics*, 14:47–83, 2011.
- [9] Randall Collins. *Violence: A Micro-Sociological Theory*. Princeton University Press, Princeton, NJ, 2008.
- [10] Subinay Dasgupta, Raj Kumar Pan, and Sitabhra Sinha. Phase of Ising spins on modular networks analogous to social polarization. *Physical Review E*, 80:025101, 2009.
- [11] Stephen P. Diggle, Ashleigh S. Griffin, Genevieve S. Campbell, and Stuart A. West. Cooperation and conflict in quorum-sensing bacterial populations. *Nature*, 450:411–414, 2007.
- [12] D. Dion and R. Axelrod. The further evolution of cooperation. *Science*, 242:1385–1390, 1988.
- [13] Ernst Fehr and Urs Fischbacher. The nature of human altruism. *Nature*, 425:785, 2003.
- [14] Ronald Fischer, Rohan Callander, Paul Reddish, and Joseph Bulbulia. How do rituals affect cooperation? *Human Nature*, 24:115–125, 2013.
- [15] Serge Galam, Yuval Gefen, and Yonathan Shapir. Sociophysics. *Journal of Mathematical Sociology*, 9:1–13, 1982.
- [16] Sandra González-Bailón, Javier Borge-Holthoefer, Alejandro Rivero, and Yamir Moreno. The dynamics of protest recruitment through an online network. *Scientific Reports*, 1:1–7, 2011.
- [17] Mark Granovetter. Threshold models of collective behavior. *American Journal of Sociology*, 83:1420–1443, 1978.
- [18] Nikki Jones and Geoffrey Raymond. The camera rolls: Using third-party video in field research. *Annals of the American Academy of Political and Social Science*, 642:109–123, 2012.
- [19] Sebastian M Krause, Philipp Böttcher, and Stefan Bornholdt. Mean-field-like behavior of the generalized voter-model-class kinetic ising model. *Physical Review E*, 85:031126, 2012.
- [20] Mark Levine, Paul J. Taylor, and Rachel Best. Third parties, violence, and conflict resolution. *Psychological Science*, 22:406–412, 2011.
- [21] Lasse Suonperä Liebst, Richard Philpot, Wim Bernasco, Kasper Lykke Dausel, Peter Ejbye-Ernst, Mathias Holst Nicolaisen, and Marie Rosenkrantz Lindegaard. Social relations and presence of others predict bystander intervention. *Aggressive Behavior*, 45:598–609, 2019.
- [22] Paul Luff and Christian Heath. Some technical challenges of video analysis. *Qualitative Research*, 12:255–279, 2012.
- [23] Gerald Marwell and Pamela Oliver. *The Critical Mass in Collective Action*. Cambridge University Press, Cambridge, MA, 1993.
- [24] William H. McNeill. *Keeping Together in Time: Dance and Drill in Human History*. Harvard University Press, Cambridge, MA, 1995.

- [25] E-J Milne, Claudia Mitchell, and Naydene de Lange. *Handbook of Participatory Video*. AltaMira Press, Walnut Creek, CA, 2012.
- [26] Hidetoshi Nishimori. *Statistical Physics of Spin Glasses and Information Processing*. Clarendon Press, Oxford, 2001.
- [27] Martin A. Nowak and Karl Sigmund. Evolution of indirect reciprocity. *Nature*, 437:1291–1298, 2005.
- [28] Mancur Olson. *The Logic of Collective Action*. Harvard University Press, Harvard, 1965.
- [29] Giorgio Parisi. Spin glasses and fragile glasses: Statics, dynamics, and complexity. *Proceedings of the National Academy of Sciences*, 103:7948–7955, 2006.
- [30] Matjaž Perc, Jillian J. Jordan, David G. Rand, Zhen Wang, Stefano Boccaletti, and Attila Szolnoki. Statistical physics of human cooperation. *Physics Reports*, 687:1–51, 2017.
- [31] Richard Philpot, Lasse Suonperä Liebst, Mark Levine, Wim Bernasco, and Marie Rosenkrantz Lindegaard. Would I be helped? Cross-national CCTV footage shows that intervention is the norm in public conflicts. *American Psychologist*, 75:66–75, 2020.
- [32] Dietrich Stauffer and Sorin Solomon. Ising, Schelling and self-organising segregation. *European Physical Journal B*, 57:473–479, 2007.
- [33] William B. Swann, Jolanda Jetten, Ángel Gómez, Harvey Whitehouse, and Bastian Brock. When group membership gets personal: A theory of identity fusion. *Psychological Review*, 119:441–456, 2012.
- [34] Duncan J. Watts. A simple model of global cascades on random networks. *Proceedings of the National Academy of Sciences*, 99:497–502, 2002.